Materials Characterization 144 (2018) 631–640

Contents lists available at ScienceDirect

Materials Characterization

journal homepage: www.elsevier.com/locate/matchar

Toughening mechanism of inter-critical heat-affected zone in a 690 MPa grade rack plate steel

Min Tong[a,b], Xinjie Di[a,b], Chengning Li[a,b,*], Dongpo Wang[a,b,c]

[a] School of Materials Science and Engineering, Tianjin University, Tianjin 300350, China
[b] Tianjin Key Laboratory of Advanced Joining Technology, Tianjin 300350, China
[c] State Key Laboratory of Metal Material for Marine Equipment and Application, Anshan 114009, China

ARTICLE INFO

Keywords:
690 MPa grade rack plate steel
ICHAZ
Toughness
Grain refinement
Plastic deformation
Geometrically necessary dislocations

ABSTRACT

The inter-critical heat-affected zone (ICHAZ) and fine grain heat-affected zone (FGHAZ) of a 690 MPa grade rack plate steel were simulated by Gleeble3500 simulator. The toughening mechanism of ICHAZ was clarified by analyzing microstructural characteristics and instrumental Charpy impact tests. The study showed that the ICHAZ had higher toughness than FGHAZ. And the microstructure in FGHAZ was martensite, while bainitic microstructure was obtained in ICHAZ. Both the prior austenite grain size and effective grain size of ICHAZ were smaller than that of FGHAZ, which played an important role in improving the toughness of ICHAZ. It was found that the extensive plastic deformation prior fracture in ICHAZ could consume large energy during crack initiation and propagation. The large plastic deformation capacity of ICHAZ was related to the large fraction of large-angle boundaries and low dislocation density, as well as the homogeneous distribution of local strain and geometrically necessary dislocations.

1. Introduction

690 MPa grade rack plate steels (equivalent to ASTM A517Gr.Q MOD) possessing high strength and enhanced low-temperature toughness have been extensively used for the building of legs in offshore platforms [1,2]. Welding is a fundamental technology in the fabrication and repair of structures in the offshore industry. Significant microstructure change would arise in the heated affected zone (HAZ) under the welding thermal cycle effect, which consequently cause deterioration of mechanical properties [3]. Therefore, mechanical properties (especially the toughness) of HAZ are crucial for the service safety of the whole platform.

The HAZ is a narrow zone that includes various microstructures, which can further be divided into several sub HAZs with different peak temperatures, including coarse grained HAZ (CGHAZ), fine grain heat-affected zone (FGHAZ), inter-critical HAZ (ICHAZ) and so on [4,5]. The microstructure-property relationships in these sub-HAZs have been extensively studied in recent years. For most steels, the FGHAZ has the best strength and toughness due to the grain refinement with the peak temperature slightly above Ac3 [6,7]. However, the CGHAZ usually is the local brittle zone (LBZ) that is the weakest location in the weld joint [8]. Numerous studies attributed the low toughness in CGHAZ to the considerable growth of prior austenite grains at a peak temperature much higher than Ac3, as well as the formation of hard microstructures (i.e. martensite and M-A constituents) [9–11].

In contrast to FGHAZ and CGHAZ, few studies were focused on the properties of ICHAZ, and the toughness mechanism of in ICHAZ is still controversial [12,13]. Since the peak temperature is between Ac1 and Ac3, partial austenite transformation occurs in ICHAZ. Some studies suggested that the ICHAZ was also a low toughness region, and most of them simply discussed the effect of M-A components on the toughness [12,14]. It has been demonstrated that the transformation products in the ICHAZ are varied concerning different steels [15]. The ICHAZ of the ×80 pipeline steel is consisted of ferrite, bainite, and M–A constituents [12]. However, the microstructure in the ICHAZ of HQ130 steel is a mixture of fine lath martensite and granular bainite [13]. In steelmaking industries, it has been demonstrated that the inter-critical heat treatment (IHT) can increase the low-temperature toughness by microstructure refinement [16,17]. If the initial microstructure is favorable, such as martensite and bainite, grain refinement could be obtained by single-cycle rapid austenization through the Ac1 and Ac3 range [18]. Welding thermal cycle is characterized by rapid heating, high peak temperature and fast cooling rate and the single welding thermal cycle can be regarded as rapid heat treatment. The question then arises as to whether the grain refinement and excellent toughness would occur with the inter-critical welding thermal cycle, an aspect

* Corresponding author at: School of Materials Science and Engineering, Tianjin University, Tianjin 300350, China.
E-mail address: licn@tju.edu.cn (C. Li).

https://doi.org/10.1016/j.matchar.2018.08.021
Received 8 May 2018; Received in revised form 12 August 2018; Accepted 12 August 2018
Available online 13 August 2018
1044-5803/ © 2018 Elsevier Inc. All rights reserved.

Table 1
Chemical composition of A517Q steel (wt%).

Element	C	Si	Mn	Cr	Mo	Ni	Cu	Nb	Al	Ti	V	B
	0.141	0.290	1.22	0.491	0.555	2.82	0.0473	0.0133	0.0661	0.0040	0.0028	0.0022

that does not seem to have been documented or explored.

In the present paper, the ICHAZ of 690 MPa grade rack plate steel consisting of bainitic microstructure was investigated by conducting weld thermal cycle simulation and instrumental Charpy impact test. In addition, FGHAZ was also investigated for the better understanding of the toughness mechanism of ICHAZ. The simulated HAZ microstructure were identified in detail by scanning electron microscopy (SEM) coupled with electron back-scatter diffraction (EBSD) analysis and transmission electron microscopy (TEM). The resultant quantitative analysis data of simulated HAZ microstructures were then correlated with the Charpy impact test results, which were discussed in terms of the fundamental to describe the toughness mechanism.

2. Experimental Procedures

The base material used in the present work was a commercial high-strength steel with thickness of 178 mm. The chemical composition of the studied material is depicted in Table 1. It was conducted by the quenching-tempering (Q-T) process: after hot rolling and cooling to the ambient temperature, the steel was austenitized at ~900 °C followed by quenching, and then tempered at ~600 °C for ~5 h. The yield strength, ultimate tensile strength and elongation of the as-received steel are 799 MPa, 877 MPa and 22.8%, respectively.

The welding thermal simulation was conducted using a Gleeble 3500 simulator. In order to estimate the Ac1 and Ac3 temperature, specimens with cylindrical form Φ3.0 mm × 60.0 mm were heated to 1350 °C at a heating rate of 200 °C/s. The measured Ac1 point and Ac3 point were ~745 °C and ~850 °C, respectively. Specimens with dimension of 11.0 mm × 11.0 mm × 76.0 mm were cut from the middle of the as-received rack plate steel. To simulate the ICHAZ and FGHAZ, the specimens were heated to the peak temperatures of 800 °C and 1050 °C at the rate of 200 °C/s, respectively. After holding for 1.0 s at the peak temperature, they were cooled to 200 °C with $t_{8/5}$ of 20 s, corresponding to the heat input of 3.6 kJ/mm. Additionally, the dilatometer curves of the specimens during cooling of welding thermal cycle were examined by Gleeble simulator to investigate the transformation behaviors.

Simulated HAZ with width of ~2 mm was obtained near the monitoring thermocouples after the thermal simulation test, and the metallographic specimen was taken from the center of simulated specimen

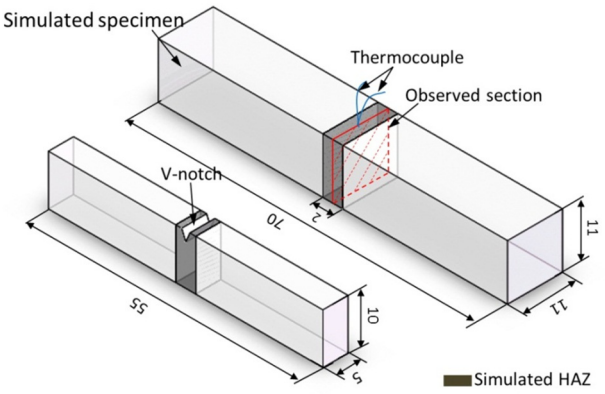

Fig. 1. Schematic depicting the geometry of simulated specimen, the observed section of metallographic specimen and the dimensions of the Charpy impact test specimen extracted from the simulated specimen.

(Fig. 1). The metallographic specimens were ground, polished and etched with nital 4%. Microstructural analyses were performed by SEM (JEOL JSM7500F). Some of them were also electrochemically polished and analyzed using EBSD in the SEM. The electro-polishing was conducted using 90 ml CH_3COOH + 10 ml $HClO_4$ solution at 25 V and ambient temperature. Orientation mapping for the EBSD data were performed with a 150 nm step size, and the data were analyzed by TSL-OIM software. Thin foils for TEM observation were prepared by twin-jet electro-polishing in a solution of 95 ml CH_3COOH + 5 ml $HClO_4$ at 75 V and −25 °C and examined using PHILIPS CM200 transmission electron microscopy. In addition, the optical microstructures of the simulated specimens were observed after etching by the saturated picric acid. The prior austenite grain (PAG) sizes were measured by the line intercept method.

The X-ray diffraction (XRD) test was performed to estimate the dislocation density. The diffraction profiles of the (110), (200), (211), (220) reflections were measured using a conventional diffractometer (D8 advanced XRD) with Cu-Kα radiation (λ = 1.542 Å) operating at 40 kV and 40 mA at a scan speed of 1.5°·min^{-1}. The dislocation density can be calculated according to the MWH equation [19,20].

$$\Delta K \cong \frac{0.9}{D} + bM\sqrt{\frac{\pi}{2}\rho}\left(K\overline{C}^{\frac{1}{2}}\right) \quad (1)$$

where $\Delta K = \cos\theta(\Delta 2\theta)/\lambda$, $K = 2\sin\theta/\lambda$, θ is the diffraction angle, λ is the wavelength of the X-rays, D is a size parameter, b is the magnitude of the Burgers vector (b = 0.283 nm), ρ is dislocation density, M is a constant depending on the effective outer cut-off radius of dislocations, and $\overline{C}$ is the average contrast factors of the dislocations for different reflections. ΔK is the full widths at half maximum (FWHM) that obtained directly from XRD results.

The hardness values of the thermal simulation specimens were measured under the load of 1 kg and dwell time of 15 s using a Vickers hardness tester (HVA-10A). The instrumental Charpy impact tests were operated at −40 °C using a 1/2 sub-size standard 2.0 mm central V-notch specimens (55.0 mm × 10.0 mm × 5.0 mm) according to ASTM E23 [21]. The geometries of simulated specimen and the Charpy impact test specimens extracted from the simulated specimen are illustrated in Fig. 1. Note that the mechanical notch was cut within the effective zone of simulated HAZ. For each Charpy impact test condition, three specimens were used to calculate the average values and standard deviations of impact absorbed energy. The fracture surfaces of Charpy impact tests specimens were subsequently examined by SEM.

3. Results and Discussion

3.1. Mechanical Properties and Fracture Morphologies

The Vickers hardness and Charpy impact absorbed energy of the BM, ICHAZ and FGHAZ are shown in Fig. 2. As can be seen from Fig. 2a, the hardness of the ICHAZ and FGHAZ are almost at the same level, with the average value of ~399 HV1 and ~407 HV1, respectively. And their hardness are both higher than that of BM (~267 HV1). In addition to the higher hardness, the toughness of ICHAZ and FGHAZ are also improved compared with the BM, and the ICHAZ exhibits a better combination of strength and toughness than FGHAZ. As shown in Fig. 2b, the ICHAZ has the highest toughness of 88 J and FGHAZ has the moderate toughness of 46 J.

The impact load curves as well as impact absorbed energy cures were recorded by instrument. The typical impact load curves can be

Download English Version:

https://daneshyari.com/en/article/7969161

Download Persian Version:

https://daneshyari.com/article/7969161

Daneshyari.com